*Original Article*

# Ethanolic extract of *Halymenia durvillei* induced G2/M arrest and altered the levels of cell cycle regulatory proteins of MDA-MB-231 triple-negative breast cancer cells

**Rapeewan Settacomkul[1,2], Kant Sangpairoj[3], Suttinee Phuagkhaopong[4], Krai Meemon[5], Nakorn Niamnont[6], Prasert Sobhon[5], and Pornpun Vivithanaporn[2,*]**

[1]*Faculty of Science, Mahidol University, Bangkok 10400, Thailand.*
[2]*Chakri Naruebodindra Medical Institute, Faculty of Medicine Ramathibodi Hospital, Mahidol University, Samut Prakan 10540, Thailand.*
[3]*Division of Anatomy, Department of Preclinical Science, Faculty of Medicine, Thammasat University, Pathum Thani 12120, Thailand.*
[4]*Department of Pharmacology, Faculty of Medicine, Chulalongkorn University, Bangkok 10330, Thailand.*
[5]*Department of Anatomy, Faculty of Science, Mahidol University, Bangkok 10400, Thailand.*
[6]*Department of Chemistry, King Mongkut's University of Technology Thonburi, Bangkok 10140, Thailand.*

## *Abstract*

**Background and purpose:** The GC-MS analysis reported *n*-hexadecanoic acid or palmitic acid as a major component of the ethanolic extract of *Halymenia durvillei* (HDET). This compound shows cytotoxic effects against various human cancer cells. The present study investigated the effect of HDET on the viability and proliferation of MDA-MB-231, a triple-negative breast cancer (TNBC) cell line.
**Experimental approach:** Cell proliferation and cell cycle analysis were determined by flow cytometry and cell cycle regulatory protein expression levels were then determined by Western blotting. The presence of reactive oxygen species (ROS) was evaluated by dichlorofluorescein, followed by analyzing changes in gene expression of antioxidant enzymes using a real-time polymerase chain reaction.
**Findings/Results:** HDET dose-dependently reduced cell viability with the 50% inhibitory concentration (IC$_{50}$) of 269.4 ± 31.2 µg/mL at 24 h. The cell proliferation assays showed increased succinimidyl ester fluorescent intensity after treatment with ≥ 100 µg/mL of HDET, indicating the inhibition of cell proliferation. Cell cycle analysis using propidium iodide staining showed an increased percentage of cells in the G2/M phase. HDET also decreased the levels of cell cycle regulatory proteins including cyclin D1 and increased the level of p21. HDET promoted oxidative stress by increasing ROS levels along with the reduction of catalase expression. However, HDET did not induce apoptosis and caspase activation in TNBC cells.
**Conclusion and implications:** These findings suggest that HDET which is rich in palmitic acid may serve as a potential therapeutic agent to target TNBC *via* arrest cell cycle progression at the G2/M phase.

*Keywords:* Cell cycle arrest; Red algae; Triple-negative breast cancer.

## INTRODUCTION

Triple-negative breast cancer (TNBC) is the most aggressive subtype of breast cancer with no specific targeted therapy and a high resistance rate (1). The major components extracted from red algae, including sulfated oligosaccharides (2), n-hexadecanoic acid (palmitic acid) (3), and sulfated polysaccharide (4), exert a marked anticancer effect. Red algae extracts show good clinical anticancer effects on lung cancer, glioblastoma, oral cancer, and leukaemia (2-5), but only a few studies have reported its effect on breast cancer. The sulfated polysaccharide isolated from the red alga *Laurencia papillosa* induces cell cycle arrest in MDA-MB-231 TNBC cell lines (4).

*Corresponding author: P. Vivithanaporn
Tel: +66-28391817, Fax: +66-22011611
Email: pornpun.viv@mahidol.ac.th

Recently, an epidemiological study has provided evidence that the intake of the red alga *Porphyra sp.* in the diet correlates with lower breast cancer risk in Korean women (6).

*Halymenia durvillei* (HD) is an edible red alga found on the coastline of the Indo-West Pacific region and consumed as food. Previous investigations have shown that HD has potential anti-viral, anti-microbial, antioxidant, and anticancer effects (7-9). HD shows a greater inhibitory effect on the growth of HT-29 human colorectal adenocarcinoma cells, A549 human lung carcinoma cells, AGS human gastric adenocarcinoma cells, and PC3 human prostate cancer cells compared with other red algae species (*Eucheuma striatum* and *Kappaphycus alvarezzi*) (10). The present study investigated the *in vitro* effect of HD ethanolic extract (HDET) on the viability and proliferation of MDA-MB-231, a human TNBC cell line.

## MATERIALS AND METHODS

### Cell line

MDA-MB-231 cell line was purchased from American Type Culture Collection (ATCC) and cultured in Dulbecco's modified eagle's medium (DMEM, Gibco, USA) with 1% penicillin-streptomycin (Merck, USA) and 10% fetal bovine serum (FBS, Gibco, USA). Cells were maintained at 37 °C in a 5% $CO_2$ humidified atmosphere.

### Algae extraction
#### Preparation of extracts

The red algae, HD, were provided and authenticated by Phetchaburi Coastal Fisheries Research and Development Center, Phetchaburi province, Thailand. The voucher number was SPFR16040. Samples (1.1 kg) were dried and macerated successively with ethanol (EtOH, 5 L) at room temperature for 7 days .The solvent was evaporated by rotary evaporation at 40 °C to yield the EtOH extract. Then, the EtOH extract (44.5 g) was partitioned with *n*-hexane until colorless to remove chlorophyll and chlorophyll-free EtOH extract was designated as HDET. The extract was dissolved in dimethyl sulfoxide (DMSO). The maximum concentration of the final DMSO concentration was 0.25% (v/v).

### Gas chromatography-mass spectrometry

The phytochemical investigation of HDET was performed on gas chromatography-mass spectrometry (GC-MS) equipment (Agilent Technologies 7890B, USA). Experimental conditions of the GC-MS system were set as follows: HP-5 column 30 m × 0.24 mn i.d with 0.25 μm film thickness. The flow rate of the mobile phase (carrier gas: He) was set at 1.0 mL/min. In the gas chromatography part, the temperature program (oven temperature) was 50 ℃ raised to 250 ℃ at 5 ℃/min and the injection volume was 1 μL. Samples dissolved in chloroform were run fully at a range of 50-400 m/z and the results were compared using the Wiley Spectral library search program NIST MS search 2.0.

### Cell viability assay

Cells were plated in 96-well plates at $1 \times 10^4$ cells/well and cultured until 70-80% confluency. Then, cells were treated with HDET at the final concentrations of 100 to 1,000 μg/mL for 24 h. Negative control for each experiment was treated with DMEM plus 0.25% DMSO. After treatment, 3-(4,5-dimethylthiazol-2-yl)-2,5-diphenyltetrazolium bromide (MTT) solution (Bio Basic, Canada) was added into the well at the final concentration of 0.4 mg/mL and incubated for 2 h, following by dissolving formazan product in DMSO. The optical density was measured at 562 nm by a microplate reader (Varioskan Flash Microplate Reader, Thermo Fisher Scientific, USA).

### Cell proliferation assay

Cells were labeled by 1 μmol/L of 5(6)-carboxy-fluorescein diacetate N-succinimidyl ester (CFSE; Sigma, Germany) in a dark place at 37 °C for 10 min. After that, cells were seeded with DMEM plus 5% FBS in 6-well plates at $1 \times 10^5$ cells/well. After 24 h, cells were treated with HDET at the final concentrations of 100, 150, and 200 μg/mL. Cells retreated with the HDET once at 48 h. After 96 h, cells were trypsinized by 0.1% trypsin-ethylenediaminetetraacetic acid (EDTA) and cell lysate was collected. The level of mean fluorescence intensity (MFI) in stained cells was detected by a flow cytometer (Guava®

easyCyte, Luminex Corporation, USA). MFI of treated groups was measured and compared with the untreated control group.

## Cell cycle assay

MDA-MB-231 cells were plated with DMEM containing 10% FBS in 6-well plates at $1.2 \times 10^5$ cells/well overnight, and then cells were serum-starved for 24 h to synchronize cells into G0/G1 phase. The next day, cells were treated with HDET at the final concentrations of 100, 150, and 200 µg/mL in DMEM containing 5% FBS. After 48 h, cells were trypsinized and collected as previously described (11). Propidium iodide (PI) fluorescent intensity was analyzed by the flow cytometer.

## Western blotting

MDA-MB-231 cells were plated with DMEM containing 10% FBS in 60-mm dishes at $2.5 \times 10^5$ cells/dish overnight, and then cells were serum-starved for 24 h. Cells were treated with HDET at 100, 150, and 200 µg/mL fo r 48 h. After that, cells were washed with cold phosphate-buffered saline (PBS) and lysed by lysis buffer containing protease inhibitor cocktail as previously described (11). Bradford reagent was used to determine the concentrations of proteins in the samples. The protein samples were loaded into sodium dodecyl sulfate-polyacrylamide gels and were transferred into nitrocellulose membranes. Membranes were blocked by 5% skim milk in tris-buffered saline with 0.1% tween 20 and were blotted with antibodies detecting cell cycle regulator proteins, including cyclin D1 (cell signaling, 1:1000 dilution), p21 (cell signaling, 1:1000 dilution), and β-actin (cell signaling, 1:2000 dilution). The band density of the protein of interest was determined and normalized with β-actin as internal loading controls using ImageJ software (version 5.0).

## Dichlorodihydrofluorescein assay

MDA-MB-231 cells were plated with DMEM without phenol red in 96-well black clear bottom plates at 10,000 cells/well and cultured until 70-80% confluency. Cells were incubated in 2′,7′-dichlorofluorescin diacetate (DCFH-DA; Sigma, Germany) for 40 min in a dark place. After that, cells were treated with HDET at the final concentrations of 100, 150, and 200 µg/mL. DMSO (0.25% v/v) was used as a negative control and tert-butyl hydroperoxide (tBuOOH; Sigma, Germany) was used as a positive control. At 1, 3, and 6 h, the fluorescence intensity was determined with the excitation at 490 nm and emission at 535 nm by a microplate reader (Synergy™ Neo2 Multi-Mode Microplate Reader, BioTek Instruments, USA).

## Real-time polymerase chain reaction

MDA-MB-231 cells were plated with DMEM containing 10% FBS in 60-mm dishes at $3.5 \times 10^5$ cells/dish. At 70-80% confluency, cells were treated with HDET at 200 µg/mL and 0.25% DMSO for negative control. After 24 h, RNA extraction, complementary DNA (cDNA) synthesis, and quantitative real-time polymerase chain reaction (RT-PCR) were performed respectively as previously described (12). Gene expression of antioxidant enzymes including catalase (*CAT*), superoxide dismutase (*SOD*), glutathione peroxidase 1 (*GPx-1*), and glutathione S transferase A4 (*GST-A4*) were analyzed. The expression of the gene of interest was normalized to the expression of the housekeeping gene, glyceraldehyde-3-phosphate dehydrogenase (*GAPDH*). The forward and reverse primers are shown in Table 1. The expression of genes was reported as relative fold change (RFC) according to the $2^{-\Delta\Delta Ct}$ equation. The RFC value of DMSO-treated cells was defined as 1.

## Apoptosis assay

Cells were plated in 6-well plates at $3.5 \times 10^5$ cells/well and cultured until 70-80% confluency. Cells were treated with HDET at 200 and 500 µg/mL and DMSO (0.25% v/v) was used as a negative control. After 24 h, the supernatant was collected, and cells were washed with annexin V binding buffer and then stained with annexin V-fluorescein isothiocyanate (FITC; BD Biosciences) in darkness at room temperature for 15 min. Apoptotic cell populations were determined by the flow cytometer.

**Table 1.** Lists of primer sequences.

| Primers | Sequences |
|---------|-----------|
| *CAT* | Forward: 5'- CCATTATAAGACTGACCAGGGC-3' <br> Reverse: 5'-AGTCCAGGAGGGGTACTTTCC-3' |
| *GPx1* | Forward: 5'-TTCCCGTGCAACCAGTTTG-3' <br> Reverse: 5'-TTCACCTCGCACTTCTCGAA-3' |
| *GST-A4* | Forward: 5'-GGATCTGCTGGAACTGCTTATCAT-3' <br> Reverse: 5'-TGTCCGTGACCCCTTAAAATCTT-3' |
| *SOD1* | Forward: 5'-CTGAAGGCCTGCATGGATTC-3' <br> Reverse: 5'-CCAAGTCTCCAACATGCCTCTC-3' |
| *GAPDH* | Forward: 5'-AGCCTTCTCCATGGTGGTGAAGAC-3' <br> Reverse: 5'-CGGAGTCAACGGATTTGGTCG-3' |
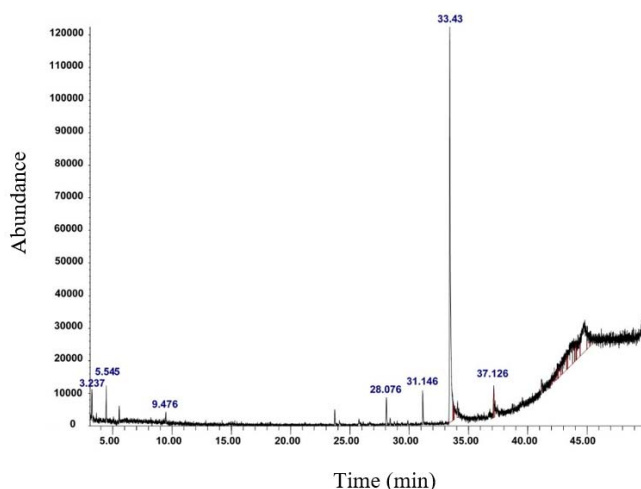


**Fig. 1.** Gas chromatography-mass spectrometry chromatogram of ethanolic extract of *Halymenia durvillei* fraction.

### Caspase 3/7 activation assay

Cells were plated and treated with the same condition of apoptosis assay. After 24 h, the supernatant was collected and cells were washed with PBS and stained with caspase solution in a dark place at 37 °C for 1 h according to the manufacturer's protocol (Guava Caspase 3/7 FAM Kit 4500-0540, Merck Millipore, USA). After that, cells were washed with apoptosis washing buffer and stained with caspase-7-AAD. The cells with activated-caspase and death cell populations were determined by the flow cytometer.

### Statistical analysis

The data were performed at least three times and presented as mean ± SEM. The comparison of two populations was performed by Student's *t*-test while multiple-sample comparisons were compared by one-way analysis 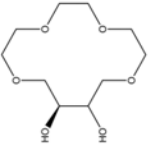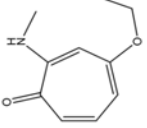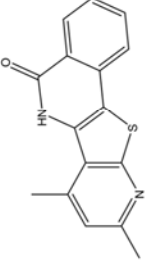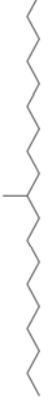of variance (ANOVA) followed by Dunnett's post-hoc test using Prism statistical analysis software (version 8.0). Differences were considered significant when the *P* value was less than 0.05.

### RESULTS

### GC-MS analysis of HD.

Seven compounds were found in the HDET fraction (Fig. 1) .These constituents and their calculated percentage peak area compositions included *n*-hexadecanoic acid, also called palmitic acid (compound 6, 79.65%), octacosyl trifluoroacetate (compound 7, 5.03%), 2-pentadecanone, 6,10,14-trimethyl (compound 5, 4.91%), (2S,13S)-12,13-dihydroxy-1,4,7,10-tetraoxacyclotetradecane (compound 1, 3.78%), 10-methylnonadecane (compound 4, 3.66%), 4-ethoxy-2-(methylamino)tropone (compound 2, 1.55%), and pyrido[2,3-b]isoquinolino[3,4]furan-5(6H)-one,7,9-dimethyl (compound 3, 1.41%) (Fig. 1 and Table 2).

**Table 2.** Compounds identified in ethanolic extract of *Halymenia durvillei* by gas chromatography-mass spectrometry.

| Compounds | RT (min) | Molecular weight | Chemical structure | Phytochemical compound | Peak area (%) | PubChem ID |
|---|---|---|---|---|---|---|
| 1 | 3.237 | 236.126 | | (2S,13S)-12,13-Dihydroxy-1,4,7,10-tetraoxacyclotetradecane | 3.78 | 14004858 |
| 2 | 5.545 | 179.094 | | 4-Ethoxy-2-(methylamino)tropane | 1.55 | 601614 |
| 3 | 9.476 | 280.067 | | Pyrido[2,3-b]isoquinolino[3,4]furan-5(6H)-one,7,9-dimethyl | 1.41 | |
| 4 | 28.076 | 282.329 | | 10-Methylnonadecane | 3.66 | 530070 |
| 5 | 31.146 | 268.277 | | 2-Pentadecanone, 6,10,14-trimethyl | 4.91 | 10408 |
| 6 | 33.43 | 256.24 | | n-Hexadecanoic acid | 79.65 | 985 |
| 7 | 37.126 | 506.431 | | Octacosyl trifluoroacetate | 5.03 | 91692945 |

### DET decreased the viability of MDA-MB-231 cells

Cells were exposed to HDET at concentrations of 100-1000 μg/mL for 24 h. The viability of untreated cells was considered 100%. Cell viability decreased concentration-dependently as the HDET concentration increased. The $IC_{50}$ of HDET at 24 h was $269.4 \pm 31.2$ μg/mL (Fig. 2).

### HDET inhibited the proliferation of MDA-MB-231 cells.

The reduced cell viability could be a result of reduced cell proliferation. The antiproliferative effect of HDET in MDA-MB-231 cells was determined by measuring the MFI of CFSE in each cell. CFSE is a non-radioactive dye that is equally divided into daughter cells in each cell division; therefore, a low MFI of CFSE represents greater cell proliferation. To minimize the effect of cytotoxicity on cell proliferation, the maximum concentration was set at a value lower than the $IC_{50}$. The doubling time of MDA-MB-231 was $26.7 \pm 8.8$ h (13). Effects of HDET on cell proliferation were evaluated at 96 h to allow 3 to 4 doubling times. A representative histogram of CFSE fluorescence intensity of cells showed the rightward shift in cells treated with increasing concentrations of HDET compared with DMSO-treated cells. The MFI increased as the HDET concentration increased, indicating that HDET inhibited the proliferation of MDA-MB-231 TNBC cells compared with DMSO-treated cells (Fig. 3).
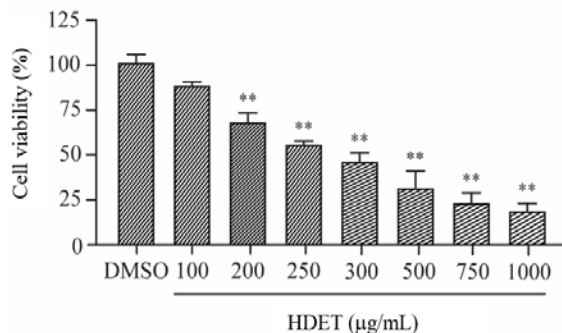


**Fig. 2.** HDET reduced the viability of MDA-MB-231 cells. Cells were treated with HDET up to 1,000 μg/mL for 24 h (n = 3). **$P < 0.01$ indicates statistically significant differences in comparison with DMSO-treated cells. HDET, Ethanolic extract of *Halymenia durvillei.*
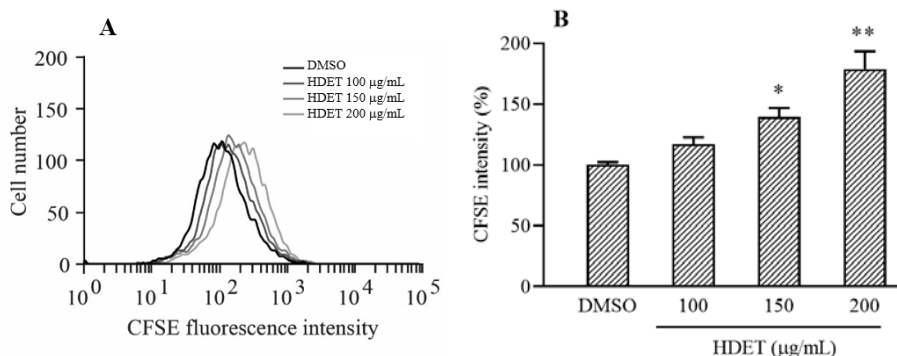


**Fig. 3.** HDET suppressed MDA-MB-231 cell proliferation. (A) A representative histogram of CFSE fluorescence intensity and (B) a bar graph showed the mean fluorescence intensity of CFSE fluorescence intensity of HDET-treated cells (n = 4). *$P < 0.05$ and **$P < 0.01$ indicate statistically significant differences in comparison with DMSO-treated cells. HDET, Ethanolic extract of *Halymenia durvillei;* CSFE, 5(6)-carboxy-fluorescein diacetate N-succinimidyl ester.

### HDET caused G2/M cell cycle arrest in MDA-MB-231 cells

The distribution of the cell cycle phases (i.e., G0/G1, S, and G2/M) was examined by flow cytometry using PI, a DNA-staining dye. MDA-MB-231 cells treated with HDET for 48 h showed an increase in the percentage of the G2/M phase with a decrease in the percentage of the G0/G1 phase compared with DMSO-treated cells (Fig. 4).

### HDET altered the expression of cell cycle regulatory proteins in MDA-MB-231 cells

The levels of cell cycle regulatory proteins including cyclin D1 and p21 were assessed by western blotting. MDA-MB-231 cells were exposed to HDET at 100, 150, and 200 μg/mL for 48 h. After HDET exposure, the expression of cyclin D1 (Fig. 5A) was downregulated, whereas the expression of p21, a cell cycle inhibitor protein (Fig. 5B), was upregulated.

### HDET altered the expression of oxidative stress-related genes in MDA-MB-231 cells

Antioxidant enzymes are key players in the human defense mechanism to counteract oxidative damage and maintain the homeostasis of cell progression. The expression of antioxidant genes, including *CAT*, *SOD*, *GST-A4*, and *GPx-1*, were determined in MDA-MB-231 cells. At 24 h, HDET decreased *CAT* mRNA levels but had no effect on the expression of *SOD*, *GST-A4*, and *GPx-1* (Fig. 6).

### HDET-induced reactive oxygen species generation in MDA-MB-231 cells

The accumulation of reactive oxygen species (ROS) causes oxidative stress and induces cell death. The cellular redox status presented as ROS generation levels after HDET treatment was measured by the DCF assays. Cells were exposed to HDET at 100, 150, and 200 μg/mL. The DCF fluorescence intensity was measured at 1, 3, and 6 h post-exposure to HDET (Fig. 7). The ROS generation levels of untreated cells were normalized to 100%. HDET increased the DCF intensity, indicating that HDET induced ROS generation in MDA-MB-231 cells.
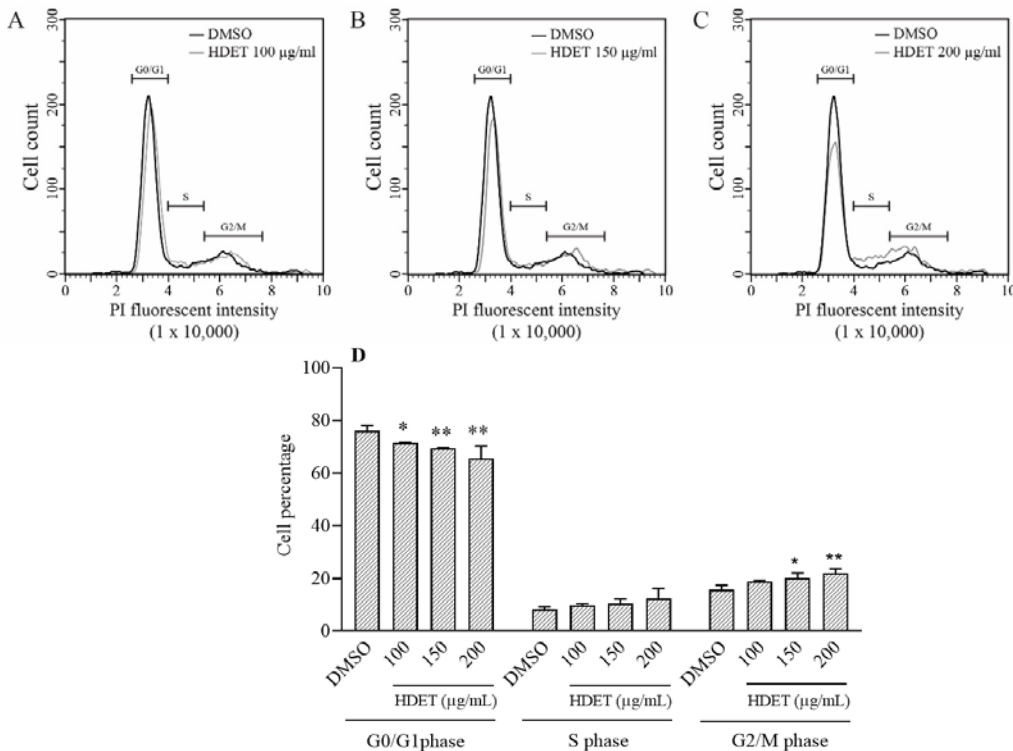


**Fig. 4.** HDET-induced G2/M cell cycle arrest in MDA-MB-231 cells. The histograms of propidium iodide intensity of cells exposed to HDET at (A) 100, (B) 150, and (C) 200 μg/mL, (D) the bar graph represents the percentage of the cells in each phase (n = 3). *$P < 0.05$ and **$P < 0.01$ indicate statistically significant differences in comparison with DMSO-treated cells. HDET, Ethanolic extract of *Halymenia durvillei*.

**Fig. 5.** HDET altered the expression of cell cycle regulator proteins in MDA-MB-231 cells. Representative blots showed expression of (A1 and A2) cyclin D1 and (B1 and B2) p21 (n = 3). *$P < 0.05$ and **$P < 0.01$ indicate statistically significant differences in comparison with DMSO-treated cells. HDET, Ethanolic extract of *Halymenia durvillei.*
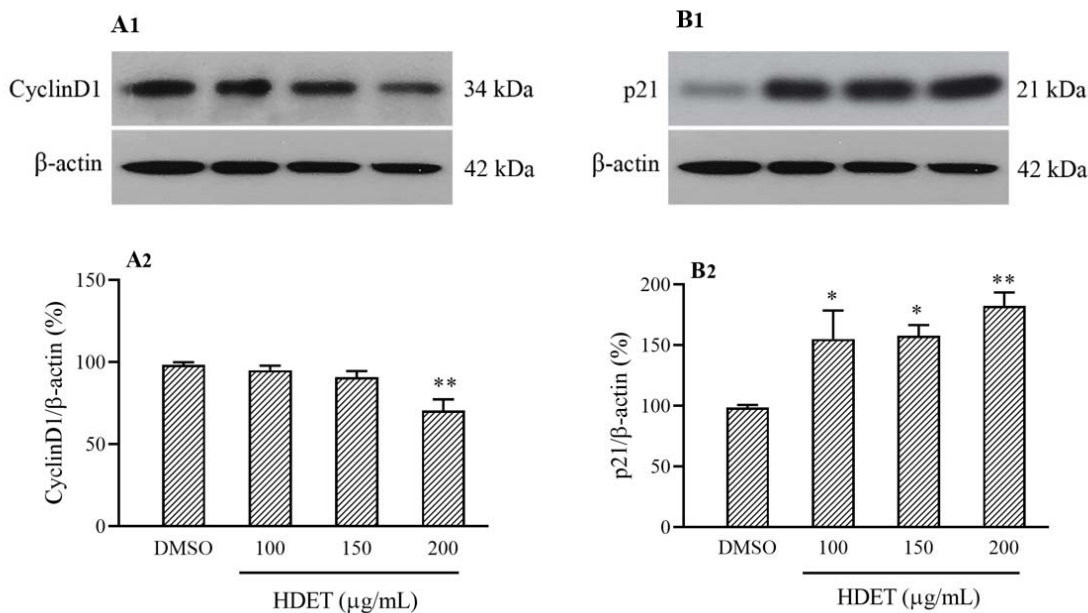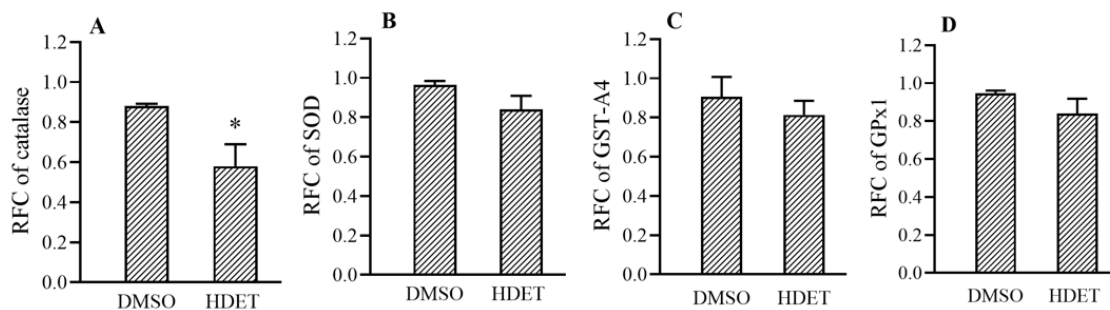


**Fig. 6.** HDET decreased the expression of catalase in MDA-MB-231 cells. Expression of oxidative stress-related genes of cells exposed to HDET at 200 µg/mL was measured (n = 3). (A) catalase, (B) *SOD*, (C) *GST-A4*, and (D) *GPx1*. *$P < 0.05$ indicates statistically significant differences in comparison with DMSO-treated cells. HDET, Ethanolic extract of *Halymenia durvillei*; RFC, Relative fold change*; SOD,* superoxide dismutase; *GST-A4;* glutathione S transferase A; *GPx1*, glutathione peroxidase 1.
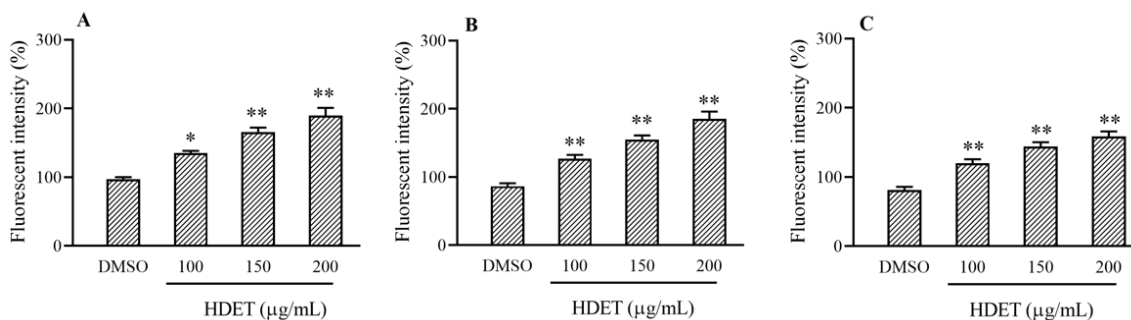


**Fig. 7.** HDET-induced ROS generation in MDA-MB-231 cells. ROS levels were measured at (A) 1, (B) 3, and (C) 6 h (n = 3). *$P < 0.05$ and **$P < 0.01$ indicate statistically significant differences in comparison with DMSO-treated cells. HDET, Ethanolic extract of *Halymenia durvillei*; ROS, reactive oxygen species.

### HDET did not induce apoptosis in MDA-MB-231 cells

The reduced cell viability could be caused by apoptosis. Herein, the percentage of apoptotic cells induced by HDET was determined by staining with annexin V-FITC, a marker of apoptosis, and measured with flow cytometry. At 24 h post-exposure, HDET at 200 µg/mL (Fig. 8A) and 500 µg/mL (Fig. 8B) did not alter the percentage of annexin V-positive cells compared with DMSO-treated cells (Fig. 8C). The apoptotic status of the cells was further determined by measuring the level of caspase 3/7 activity. At 24 h post-exposure to HDET at 200 µg/mL, the percentage of caspase3/7 activated cells did not change compared with DMSO-treated cells (Fig. 9). These results indicated that the cytotoxic effect of HDET in MDA-MB-231 cells does not involve apoptosis.
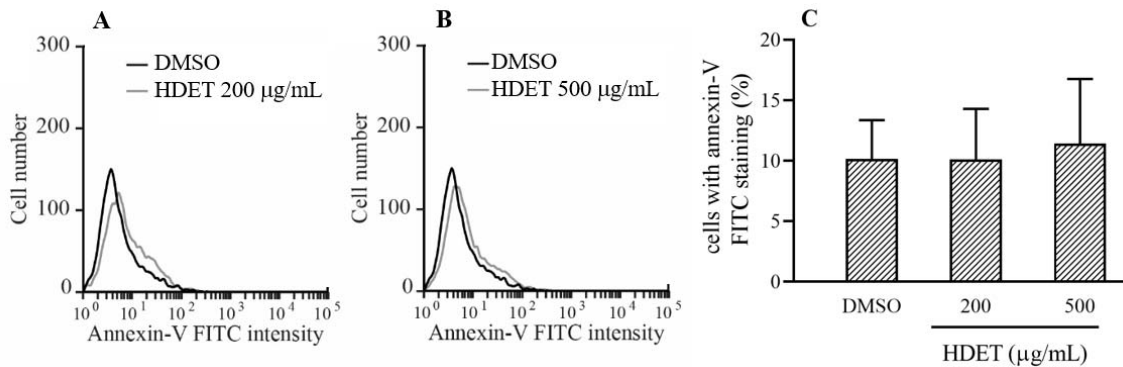


**Fig. 8.** HDET did not trigger apoptotic cell death in MDA-MB-231 cells. (A) and (B) represent histograms of annexin-V FITC intensity of HDET-treated cells and (C) A bar graph showing a similar percentage of cells with annexin-V staining in all groups (n = 4). HDET, Ethanolic extract of *Halymenia durvillei*.



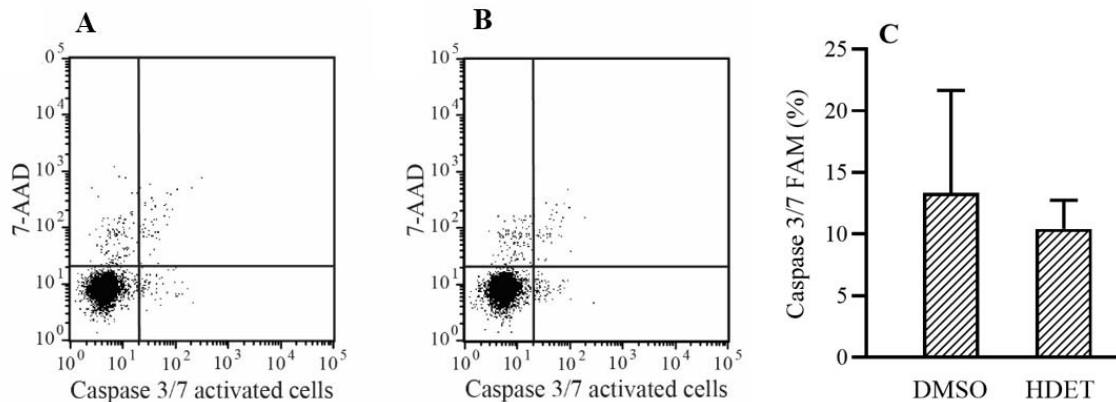**Fig. 9.** HDET at 200 µg/mL did not induce caspase 3/7 activation in MDA-MB-231 cells. Two representative dot plots showed exposure to (A) DMSO (control) and (B) 200 µg/mL HDET; (C) the bar graph showed the percentage of caspase 3/7-activated cells (n = 3). HDET, Ethanolic extract of *Halymenia durvillei*.

**DISCUSSION**

Marine algae have proven to be a promising natural source of bioactive metabolites that are believed to be beneficial for alternative cancer treatment. Here, we revealed that HDET exerts a time- and concentration-dependent cytotoxic effect on MDA-MB-231 cells. Subsequently, inhibition of the HDET-treated cells led to G2/M cell cycle arrest and concentration-dependent ROS generation.

In the present study, palmitic acid was the main compound in HDET. Over the past decade, palmitic acid, the most common saturated free fatty acid, has received a lot of attention because it can cause cell damage through lipotoxicity and apoptosis (14-16). Fatty acids are a component of the cell membrane. Changes in fatty acid components in the membrane inhibit DNA synthesis and induce membrane oxidative stress in cancer cells (17). There is evidence that palmitic acid has an inhibitory role in the development and progression of MDA-MB-231 TNBC cells by downregulating fatty acid synthase, a biomarker of poor prognosis of breast cancer patients, decreasing phosphatidylinositol-3-kinase, and promoting cytochrome c release from the mitochondria and caspase-3 activation (18-20). The hexane extract of HD showed the IC$_{50}$ value of 50.35 ± 17.72 μg/mL for MDA-MB-231 TNBC cells at 24 h (9), which is markedly lower than that of HDET (269.4 ± 31.2 μg/mL). Although the most abundant metabolite in the hexane and ethanolic extracts is *n*-hexadecanoic acid, the hexane extract contains several other compounds, including oleic acid and octadecanoic acid (stearic acid). Both oleic and stearic acids play a role in the induction of apoptosis in breast and colon cancer cells (21). The effect of HDET is close to the cytotoxic effect of the ethyl acetate extract of HD on HT-29 cells, a human colorectal adenocarcinoma cancer cell line (43% reduction with 100 μg/mL of HD) (10). Although we did not have normal human breast cell lines in the present experiment, palmitic acid extracted from *Santolina corsica* in hexane and methanol exhibits a selective growth inhibition effect on breast cancer cells (*i.e.* MCF-7 ER-positive breast cancer cells and

MDA-MB-231 TNBC cells) relative to normal breast cells (MCF-10A) (22).

Cell cycle inhibition has become an appreciated target for cancer management. Indeed, marine algal extracts have been well demonstrated to exert anti-proliferative effects on cancer cells by causing cell cycle arrest in G1, S, or G2/M phase (2,4,13,23). The sulfated oligosaccharides extracted from the red alga *Grateloupia filicina* inhibit cell proliferation in U-87 glioma cells by inducing cell cycle arrest (2). Our findings showed that HDET disrupted cell-cycle distribution by causing G2/M phase cell cycle arrest in MDA-MB-231 TNBC cells. Similarly, palmitic acid demonstrates effective anti-proliferative activity by causing cell cycle delay in G2-phase in HER2/neu-positive SKBR3 breast cancer cells (24).

There are a variety of mechanisms underlying red algal extract-induced cell cycle arrest. Cell-cycle checkpoint is a key process to regulate DNA integrity and cell-cycle transition and to induce apoptotic signaling pathways after cell stress. Algal extracts modulate the expression of potential key regulator proteins involved in cell progression. Sulfated oligosaccharide compound, G19, isolated from the red alga *G. filicina* induces G2/M phase cell cycle arrest against U-87 human glioma cells by suppressing epidermal growth factor receptor phosphorylation, leading to the increase in p21 gene expression, and the inactivation of cyclin A protein (2). Similarly, our results in MDA-MB-231 cells showed that HDET induced cell cycle retardation in the G2/M phase in a concentration-dependent manner, the mechanism of which is due in part to an increase in p21 and a reduction in cyclin D1. This could be explained by the fact that p21 is a key checkpoint protein responsible for G1 and G2 cell cycle arrest, which temporarily allows cells to survive until damage has been repaired or until cellular stress has been resolved. Consistent results have been found in resveratrol-treated human colonic adenocarcinoma cell lines (Caco-2) and aloperine-treated human colon cancer cell lines (HCT116) (25,26). Both compounds upregulate the expression of p21, which in turn, inhibits the expression of cyclin D1, resulting in the blockade of cell transition from the G2/M phase to the G1 phase.

Our study indicated that HDET increased oxidative stress. Cancer cells are more sensitive to rapid increases in ROS levels than normal cells, and many anticancer drugs selectively kill cancer cells by generating high levels of intracellular ROS (27). An increase in ROS production induced by HDET is thought to be critically involved with a reduction in antioxidant enzyme expression, feasibly *CAT* but not *SOD*, *GST-A4*, and *GPx-1*. Similar results have been reported for the sulfated polysaccharide extract from the red alga *L. papillosa* (4), sargaquinoic acid isolated from the brown alga *Sargassum heterophyllum* (13), and polysaccharides from the ethanolic extract of the brown alga *S. wightii* (28), which could promote oxidative stress in MDA-MB-231 TNBC cells. An elevated basal level of ROS has been reported to trigger the reactivation of the apoptotic program in cancer cells, promoting cancer development and metastasis. Moreover, when ROS levels surmount the cellular antioxidant defenses, they can inhibit cancer cell growth by triggering oxidative DNA damage and cell cycle arrest (29). Considering red algae, sulfated oligosaccharide compound, G19, extracts from *G. filicina* initiate oxidative stress-induced DNA damage against U-87 human glioma cells through activation of ataxia-telangiectasia-mutated phosphorylation/activated checkpoint kinase 2/p53 signaling cascade. Then, the damaged DNA activates p21 and cell cycle arrest at an intra-S phase and G2/M transition (2). Consistently, our study has demonstrated that treatment of TNBC cells with HDET rapidly induced intracellular ROS accumulation in a concentration-dependent manner before promoting cell cycle retardation at the G2/M phase. Cyclin D1 is sensitive to ROS-mediated proteolysis; therefore, it is immediately degraded when exposed to ROS, and the rapid depletion of cyclin D1 results in delayed cell cycle progression particularly at both the G1 and G2 phases through crosstalk with the checkpoint kinase 1, Cdc25 and Cdc2, DNA damage checkpoint pathway (30). Accumulating oxidative damage in the cells may be a contributing factor in HDET-induced abnormal cell cycle progression through the activation of p21 and depletion of cyclin D1. Further studies on protein levels and the activity

of antioxidant enzymes as well as the use of antioxidants to reverse the anti-proliferative effect and cell cycle arrest are required to link the role of HDET-induced oxidative stress and anti-proliferation.

## CONCLUSION

In summary, HDET exerted not only an anti-proliferative effect *via* cell cycle arrest but also oxidative stress induction in MDA-MB-231 TNBC cells. An increase in p21 and a decrease in cyclin D1 protein expression after treatment of HDET may contribute to the G2/M cell cycle arrest. Thus, our findings raise the possibility that HDET could be a potential natural alternative or a complementary therapy for TNBC.

*Conflict of interest statement*
The authors declared no conflict of interest in this study. The funders had no role in the design of the study; in the collection, analyses, or interpretation of data; in the writing of the manuscript, or in the decision to publish the results.

*Authors' contributions*
K. Sangpairog, K. Meemon, P. Sobhon, and P. Vivithanaporn contributed to the conceptualization. R; Settacomkul, S. Phuagkhaopong, and N. Niamnont were responsible for data acquisition and analysis; R. Settacomkul, K. Sangpairoj, S. Phuagkhaopong, and P. Vivithanaporn prepared the original draft of the manuscript; R. Settacomkul, S. Phuagkhaopong, and P. Vivithanaporn performed manuscript editing and review. All authors approved the final revision of the article.

## REFERENCES

1. Isakoff SJ. Triple-negative breast cancer: role of specific chemotherapy agents. Cancer J. 2010;16(1):53-61.
DOI: 10.1097/PPO.0b013e3181d24ff7.

2. Liu H, Zhou L, Shi S, Wang Y, Ni X, Xiao F, *et al*. Oligosaccharide G19 inhibits U-87 MG human glioma cells growth *in vitro* and *in vivo* by targeting epidermal growth factor (EGF) and activating p53/p21 signaling. Glycobiology. 2014;24(8): 748-765.
DOI: 10.1093/glycob/cwu038.

3. Harada H, Yamashita U, Kurihara H, Fukushi E, Kawabata J, Kamei Y. Antitumor activity of palmitic acid found as a selective cytotoxic substance in a marine red alga. Anticancer Res. 2002;22(5): 2587-2590.
PMID:12529968.

4. Murad H, Hawat M, Ekhtiar A, AlJapawe A, Abbas A, Darwish H, *et al*. Induction of G1-phase cell cycle arrest and apoptosis pathway in MDA-MB-231 human breast cancer cells by sulfated polysaccharide extracted from *Laurencia papillosa*. Cancer Cell Int. 2016;16:39.
DOI: 10.1186/s12935-016-0315-4.

5. Back SA, Tuohy TM, Chen H, Wallingford N, Craig A, Struve J, *et al*. Hyaluronan accumulates in demyelinated lesions and inhibits oligodendrocyte progenitor maturation. Nat Med. 2005;11(9): 966-972.
DOI: 10.1038/nm1279.

6. Yang YJ, Nam SJ, Kong G, Kim MK. A case-control study on seaweed consumption and the risk of breast cancer. Br J Nutr. 2010;103(9):1345-1353.
DOI: 10.1017/S0007114509993242.

7. Tassakka ACMA, Sumule O, Massi MN, Sulfahri, Manggau M, Iskandar IW, *et al*. Potential bioactive compounds as SARS-CoV-2 inhibitors from extracts of the marine red alga. Arab J Chem. 2021;14(11):103393.
DOI: 10.1016/j.arabjc.2021.103393.

8. Shah MD, Venmathi Maran BA, Shaleh SRM, Zuldin WH, Gnanaraj C, Yong YS. Therapeutic potential and nutraceutical profiling of north bornean seaweeds: a review. Mar Drugs. 2022;20(2):101,1-23.
DOI: 10.3390/md20020101.

9. Sangpairoj K, Settacomkul R, Siangcham T, Meemon K, Niamnont N, Sornkaew N, *et al*. Hexadecanoic acid-enriched extract of *Halymenia durvillei* induces apoptotic and autophagic death of human triple-negative breast cancer cells by upregulating ER stress. Asian Pacific J Trop Biomedicine. 2022;12(3):132-140.
DOI: 10.4103/2221-1691.338922.

10. Miranda M, Chiou CT, Tayo LL, Hsieh CL, Tsai PW. *In vitro* anticancer activities of selected Philippine seaweeds against several cancer cell lines. Plant Cell Biotechnol Mol Biol. 2021:22(5-6);108-114.

11. Piromkraipak P, Parakaw T, Phuagkhaopong S, Srihirun S, Chongthammakun S, Chaithirayanon K, et al. Cysteinyl leukotriene receptor antagonists induce apoptosis and inhibit proliferation of human glioblastoma cells by downregulating B-cell lymphoma 2 and inducing cell cycle arrest. Can J Physiol Pharmacol. 2018;96(8):798-806.
DOI: 10.1139/cjpp-2017-0757.

12. Phuagkhaopong S, Ospondpant D, Kasemsuk T, Sibmooh N, Soodvilai S, Power C, et al. Cadmium-induced IL-6 and IL-8 expression and release from astrocytes are mediated by MAPK and NF-kappaB pathways. Neurotoxicology. 2017;60:82-91.
DOI: 10.1016/j.neuro.2017.03.001.

13. de la Mare JA, Lawson JC, Chiwakata MT, Beukes DR, Edkins AL, Blatch GL. Quinones and halogenated monoterpenes of algal origin show anti-proliferative effects against breast cancer cells in vitro. Invest New Drugs. 2012;30(6):2187-2200.
DOI: 10.1007/s10637-011-9788-0.

14. Ford JH. Saturated fatty acid metabolism is key link between cell division, cancer, and senescence in cellular and whole organism aging. Age (Dordr). 2010;32(2):231-237.
DOI: 10.1007/s11357-009-9128-x.

15. Listenberger LL, Han X, Lewis SE, Cases S, Farese RV, Ory DS, *et al*. Triglyceride accumulation protects against fatty acid-induced lipotoxicity. Proc Natl Acad Sci USA. 2003;100(6):3077-3082.
DOI: 10.1073/pnas.0630588100.

16. Belosludtsev K, Saris NE, Andersson LC, Belosludtseva N, Agafonov A, Sharma A, *et al*. On the mechanism of palmitic acid-induced apoptosis: the role of a pore induced by palmitic acid and $Ca^{2+}$ in mitochondria. J Bioenerg Biomembr. 2006;38(2):113-120.
DOI: 10.1007/s10863-006-9010-9.

17. Koundouros N, Poulogiannis G. Reprogramming of fatty acid metabolism in cancer. Br J Cancer. 2020;122(1):4-22.
DOI: 10.1038/s41416-019-0650-z.

18. Hardy S, Langelier Y, Prentki M. Oleate activates phosphatidylinositol 3-kinase and promotes proliferation and reduces apoptosis of MDA-MB-231 breast cancer cells, whereas palmitate has opposite effects. Cancer Res. 2000;60(22):6353-6358.
PMID:11103797.

19. Al-Bahlani S, Al-Lawati H, Al-Adawi M, Al-Abri N, Al-Dhahli B, Al-Adawi K. Fatty acid synthase regulates the chemosensitivity of breast cancer cells to cisplatin-induced apoptosis. Apoptosis. 2017;22(6):865-876.
DOI: 10.1007/s10495-017-1366-2.

20. Hardy S, El-Assaad W, Przybytkowski E, Joly E, Prentki M, Langelier Y. Saturated fatty acid-induced apoptosis in MDA-MB-231 breast cancer cells. A role for cardiolipin. J Biol Chem. 2003;278(34):31861-31870.
DOI: 10.1074/jbc.M300190200.

21. Biswas P, Datta C, Rathi P, Bhattacharjee A. Fatty acids and their lipid mediators in the induction of cellular apoptosis in cancer cells. Prostaglandins Other Lipid Mediat. 2022;160:106637.
DOI: 10.1016/j.prostaglandins.2022.106637.

22. Bonesi M, Brindisi M, Armentano B, Curcio R, Sicari V, Loizzo MR, *et al*. Exploring the anti-proliferative, pro-apoptotic, and antioxidant properties of *Santolina corsica* Jord. & Fourr. (Asteraceae). Biomed Pharmacother. 2018;107:967-978.
DOI: 10.1016/j.biopha.2018.08.090.

23. Yeh CC, Yang JI, Lee JC, Tseng CN, Chan YC, Hseu YC, *et al*. Anti-proliferative effect of methanolic extract of *Gracilaria tenuistipitata* on oral cancer cells involves apoptosis, DNA damage, and oxidative stress. BMC Complement Altern Med. 2012;12:142,1-9.
   DOI: 10.1186/1472-6882-12-142.
24. Baumann J, Wong J, Sun Y, Conklin DS. Palmitate-induced ER stress increases trastuzumab sensitivity in HER2/neu-positive breast cancer cells. BMC Cancer. 2016;16:551,1-15.
   DOI: 10.1186/s12885-016-2611-8.
25. Zhang L, Zheng Y, Deng H, Liang L, Peng J. Aloperine induces G2/M phase cell cycle arrest and apoptosis in HCT116 human colon cancer cells. Int J Mol Med. 2014;33(6):1613-1620.
   DOI: 10.3892/ijmm.2014.1718.
26. Wolter F, Akoglu B, Clausnitzer A, Stein J. Downregulation of the cyclin D1/Cdk4 complex occurs during resveratrol-induced cell cycle arrest in colon cancer cell lines. J Nutr. 2001;131(8): 2197-2203.

27. DOI: 10.1093/jn/131.8.2197.
27. Kim SJ, Kim HS, Seo YR. Understanding of ROS-inducing strategy in anticancer therapy. Oxid Med Cell Longev. 2019;2019:5381692,1-13.
   DOI:10.1155/2019/5381692.
28. Vaikundamoorthy R, Krishnamoorthy V, Vilwanathan R, Rajendran R. Structural characterization and anticancer activity (MCF7 and MDA-MB-231) of polysaccharides fractionated from brown seaweed Sargassum wightii. Int J Biol Macromol. 2018;111:1229-1237.
   DOI: 10.1016/j.ijbiomac.2018.01.125.
29. Boonstra J, Post JA. Molecular events associated with reactive oxygen species and cell cycle progression in mammalian cells. Gene. 2004;337: 1-13.
   DOI: 10.1016/j.gene.2004.04.032.
30. Pyo CW, Choi JH, Oh SM, Choi SY. Oxidative stress-induced cyclin D1 depletion and its role in cell cycle processing. Biochim Biophys Acta. 2013;1830(11):5316-5325.
   DOI: 10.1016/j.bbagen.2013.07.030.